

Analysis Methods on Imaging Endothelial Adaptation Under Flow

Kelsey Q. Snider^a, Ramneek Kaur^b, Brian Helmke, PhD^{c,1}

^a UVA Department of Biomedical Engineering, Undergraduate

^b UVA Department of Biomedical Engineering, Undergraduate

^c UVA Department of Biomedical Engineering, Associate Professor

¹ Correspondence: helmke@virginia.edu, P.O. Box 800759 Charlottesville VA 22903, (434) 924-6460

Word Count: 4282

Figure(s): 10

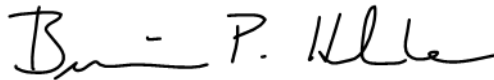
Table(s): 0

Equation(s): 0

Supplement(s): 0

Reference(s): 18

Approved



Date

5/6/25

Dr. Brian P. Helmke, Department of Biomedical Engineering

Analysis Methods on Imaging Endothelial Adaptation Under Flow

Abstract

Cerebral cavernous malformations (CCM) are mulberry-like structures in cerebral veins, formed from clusters of small blood vessels in the central nervous system. When they form, the endothelial permeability in the blood-brain barrier is increased, as a result of disrupted cell-to-cell junctions, leading to a greater risk of neurological disorders. The identified problem with this disease is that there are few current effective treatments and no methods of prevention due to a lack of information on the disease mechanism. However, it is known that endothelial cells adapt to flow, and there is a great need for quantitative analysis to assess the structural integrity of cells involved in CCM. To achieve this, we developed an image analysis technique to document and analyze cellular shape change and alignment in response to flow. First, we simulated the conditions of cerebral vein blood flow with a parallel-plate flow chamber by exposing cells to flow for 24 hours. Following this, f-actin was stained to visualize its morphology. Our image analysis technique involved processing microscopic images using bandpass filtering and binarization to identify cells. An algorithm was then employed to measure the angle of alignment of individual cells relative to the direction of flow, and these measurements were plotted in histograms for pre- and post-flow comparison. To validate the observed changes, elongation ratios were found to verify a distinct shape change. Our findings demonstrated that endothelial cells would adapt to flow and align in the direction of the applied shear stress. This image analysis technique provides a quantitative method for assessing endothelial cell adaptation to flow, laying the groundwork for future investigations into the effects of varying hemodynamic conditions on endothelial behavior in both healthy and diseased states.

Keywords: cerebral cavernous malformations, parallel-plate flow system, image analysis, alignment

Introduction

Cerebral cavernous malformations (CCMs) are a genetic neurovascular disease, characterized by the improper development of small blood vessels in the brain, resulting in leaky, pocket-shaped lesions. These lesions are characterized by impaired blood-brain barrier function, which can lead to major neurological problems and cerebral hemorrhage¹. 1 in 500 people have at least one CCM present, which can lead to inflammation, seizures, headaches, and strokes². However, 25% of people will not develop symptoms. Without the development of symptoms, people with CCM will live their lives unaware that they have this disease, until a condition occurs where interventional treatments are needed. Current treatment methods include prescribing medication to treat symptoms, MRI monitoring of lesion development, and invasive surgery to remove the malformed blood vessels if the situation requires it³. The lack of effective treatment methods is due to there being a lack of information known about the disease mechanism of CCM and how endothelial cells are affected.

One of the three genes responsible for CCM, KRIT-1, produces a loss-of-function mutation⁴. Even though this gene is linked to CCM, its role in the cell signaling pathways that regulate endothelial behavior, and

morphology is not well understood. Shear stress from blood flow has been found to play a role in regulating signaling pathways, either through activation or inhibition, which then impacts endothelial function. In a study by Li et al. (2019), they discovered that in endothelial cells with silenced KRIT-1 under low fluid shear stress results in the dysregulation of over 1000 genes. This indicates that KRIT-1 plays some role in the regulation of shear stress signaling pathways related to the genes found to be dysregulated that are mechanosensors⁵. With the involvement of KRIT-1 in shear stress regulated pathways and the change in structural integrity to endothelial cells, the importance of a quantitative image analysis method becomes clear. Lesion formation is theorized to result from the abnormal shear stress response of the endothelial layer; therefore, we created a technique to analyze the response of cells to shear stress based on their morphology to better understand this possible connection⁵. We utilized two aims to do this: identifying differences in morphology in cells under flow qualitatively and developing an algorithm to distinguish and plot each cell's alignment to flow.

The first aim was to qualitatively recognize bovine aortic endothelial cell (BAEC) alignment to flow. BAECs were chosen for initial experimentation due to their durability and

because their behavior under flow is well-characterized in previous literature, making them a good choice for a “proof of concept” model and for confirming the functionality of new protocols^{6,7}.

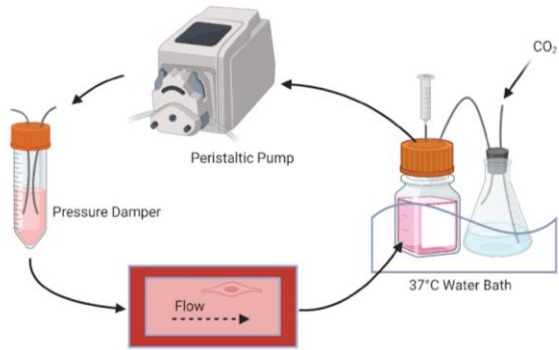


Figure 1. A diagram of the parallel-plate flow chamber setup. This system allows for shear stress to be applied to cells to study the change in morphology.

A parallel-plate flow chamber was used to identify the differences in morphology in endothelial cells with and without flow. The flow experiment allows for BAECs, cultured as a monolayer on a glass slide, to be exposed to a set shear stress. It also allows for the temperature and pH to be regulated in the system, both necessary to keep the cells alive. The use of the parallel-plate flow system (Figure 1) allows a clear visual of cell behavior and easy comparison to the control data.

Results from the previous aim provided images for the second aim of developing an algorithm to distinguish and plot each cell’s alignment to flow. The development of an image analysis technique will allow for the studying of endothelial morphology in vitro and their effect on cell structural integrity. Once created, this will help identify how the two-dimensional aspects of cerebral blood vessels play into lesion formation and characteristic leakiness.

This analysis technique, utilizing both ImageJ and MATLAB to plot cell alignment, will quantitatively show how much cells are affected by shear stress from flow. By using a band pass filter and binarizing each image of the monolayer, the cells are easily distinguishable for the alignment degree to be found. Plotting these alignment values and using elongation ratios to demonstrate shape change will verify how much a mutation, like KRIT-1, changes cell morphology and permeability.

Results

Parallel-Plate Flow Chamber

The parallel-plate flow chamber allows the user to adjust the flow rate (and therefore shear stress) and cells used, while also keeping the environment conditions constant to keep the cells alive. Cells are plated on a glass slide with a gasket and attached to the parallel-plate flow chamber. The chamber is connected through a system of tubes, to a bottle of cell medium, CO₂ for pH control, a pressure damper to protect cells from the peristaltic pump oscillation, and the peristaltic pump. Wild-type BAECs were used throughout the experiment, both as a control and in cell alignment. Healthy endothelial cells are expected to align and elongate in the direction of flow and shear stress, as shown in Figure 2 with the difference between Figure 2a and 2b.

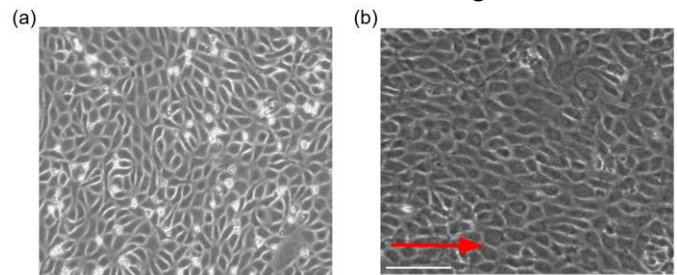


Figure 2. A comparison of wild-type BAECs before being exposed to flow (a) and after being exposed to flow (b) in the parallel-plate flow system. The red arrow on the right indicates the direction of flow. The post-flow cells are aligned and elongated in the direction of flow. Scale bar is 100µm.

Multiple experiments were done to confirm the cell alignment behavior, and the wild-type BAECs were imaged on a glass slide before and after being exposed in the chamber. There was also a control glass slide of BAECs, kept in the incubator to show there was no other manipulation to the monolayer other than flow. In the cells’ natural resting state, without being put under flow, the cells are fully confluent, round, and have a cobblestone appearance (Figure 2a). Once the cells are exposed to 24 hours of shear stress, they elongate in the direction of flow, as shown by the red arrow in Figure 2b.

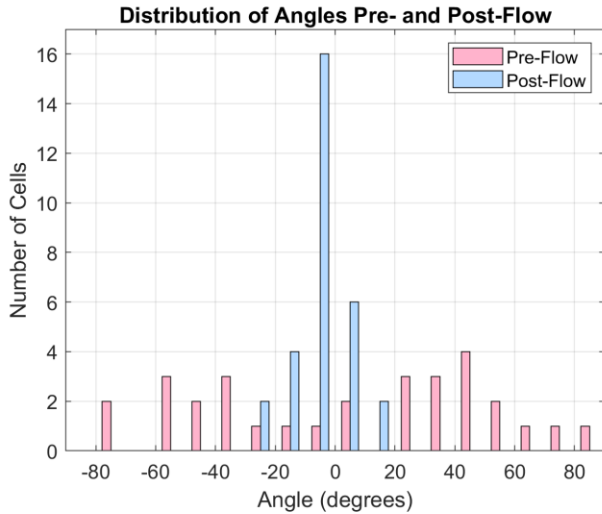


Figure 3. Histogram displaying the distribution of angle alignment of the cells relative to the direction of flow. The x-axis is angles of alignment while the y-axis is the # of cells measured. These angles were calculated manually using one image for each condition.

To quantify the alignment of the cells manually, ImageJ was used to find the angle of orientation of cells relative to the direction of flow, or the x-axis (Figure 3). The average angle of alignment for cells without flow was 4.92 degrees with a standard deviation of 47.67 degrees. The average angle of alignment for cells after being exposed to flow was -4.41 degrees with a standard deviation of 9.71 degrees. The standard deviation without flow is about 5 times greater than the standard deviation of the cells post-flow. A larger standard deviation corresponds to random orientation of cells, meaning the post-flow cells show more alignment.

For quantifying the elongation of cells, ImageJ was used to measure the major and minor axis lengths of the cells, and the elongation ratios of the cells were calculated by dividing the major axis length by the minor axis length (Figure 4). A rounder cell is expected to have an elongation ratio closer to 1 than that of a cell that has become elongated. The average major axis length of cells without flow was 26.82 μm with an average elongation ratio of 1.49. The average major axis length of cells after being exposed to flow was 54.33 μm with an average elongation ratio of 3.54. These results indicate elongation in the cells that were exposed to shear stress more than those that were not. These, in conjunction with the orientation angle calculations, reaffirmed the success in the flow experiments showing that cells orientation and shape adapt in response to flow-induced shear stress after a 24-hour period.

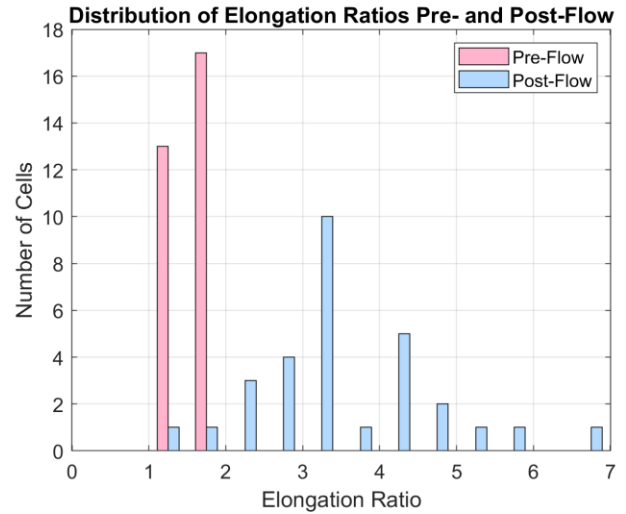


Figure 4. Histogram displaying the distribution of the cells' elongation ratios. The x-axis is the elongation ratios while the y-axis is the # of cells measured. These ratios were calculated manually using one image for each condition.

Image Analysis

ImageJ

After cells were imaged in the microscope with a 10x lens, they were uploaded into ImageJ. With the need for rapid, accurate and adaptable methods to quantify cellular alignment, the analysis process by Xu et al. (2011) was adapted for flow⁸. Once the greyscale image was uploaded, it was despeckled (Figure 5a). This removes unwanted noise by replacing each pixel with the median value in its 3x3 neighborhood. A Gaussian bandpass filter was then applied to correct uneven illumination by removing high frequency components and mitigate effects of noise other than cells by removing low frequencies (Figure 5b). This filtered out large structures (greater than 40 pixels) and small structures (less than 3 pixels) by Gaussian filtering in Fourier space. The image contrast was increased to create a stark difference between cells and background (Figure 5c). Finally, binary images were generated by Sauvola's local thresholding algorithm with a radius of 40 pixels⁹. The Open and Fill Holes operations were applied to fill in the cells completely (Figure 5d). These manipulations allow for simplified data that the MATLAB algorithm used to produce rapid results with greater accuracy in identifying the individual cells.

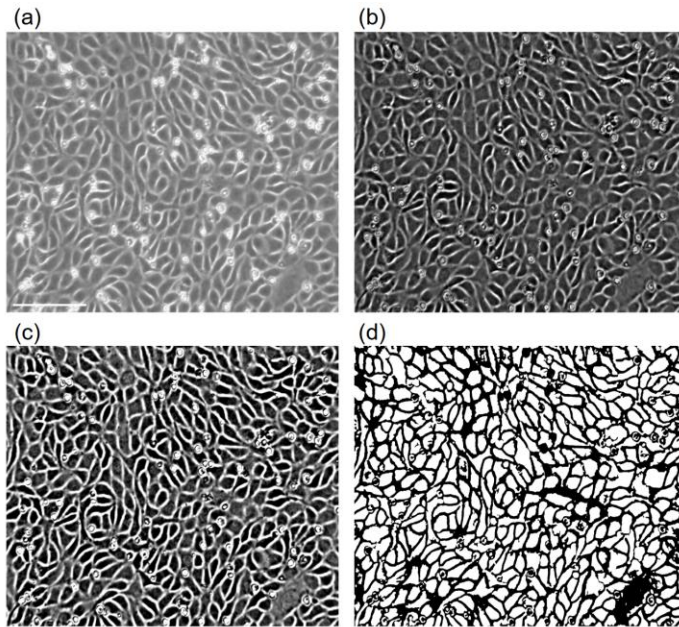


Figure 5. Steps of image analysis in ImageJ. (a) Despeckled image. (b) The image is filtered with a band-pass filter to filter out extracellular fibers and debris and correct for uneven lighting. (c) Contrast is increased to create a stark gradient from cell to background. (d) The image is binarized using Sauvola's adaptive thresholding algorithm. Open and Fill holes operation are applied. Scale bar is 100 μm .

When f-actin was stained in the fixed post-flow and control cells, the fibers were too small and not elliptical to use the method described above (Figure 6).

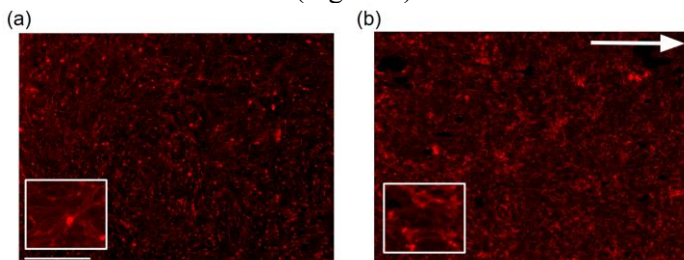


Figure 6. Fluorescence microscopy images of cell f-actin control and post-flow taken in 10x. A) Cell image of control f-actin, B) Cell image of post-flow f-actin. Scale bar is 250 μm . The white arrow on the right indicates the direction of flow.

Instead, the Directionality plugin on ImageJ was utilized to find the frequency of each angle in the image. The plugin is used to infer the preferred orientation of the fibers present in the input image and computes a table of values indicating the number of fibers in each direction. Using local gradient orientation, the gradient of the input image is calculated using a 5x5 Sobel filter. This orientation is then used to fill a table by putting the square of the gradient norm with the corresponding angle¹⁰. The angles and frequencies were plotted in MATLAB (Figure 7). Frequency is calculated by summing the histogram values within one standard deviation of the peak direction and dividing that sum by the

total histogram sum. The y-axis quantifies the "strength" of the preferred angle of alignment from the proportion of cells.

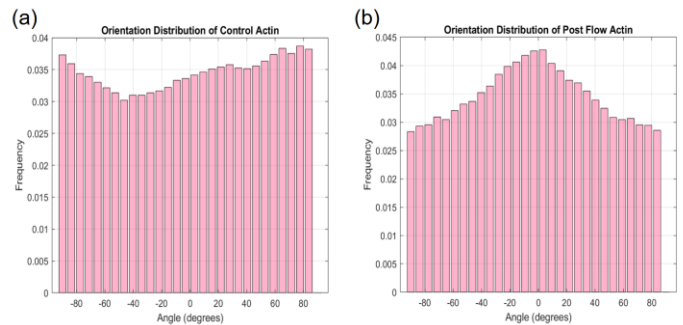


Figure 7. Angle Distribution versus frequency for f-actin images before and after flow, using values from the Directionality plugin in ImageJ. Frequency on the y-axis is the proportion of cells that are oriented at a certain angle. (a) Control f-actin angle distribution, (b) post-flow f-actin angle distribution.

MATLAB

Following the ImageJ processing to enhance the clarity of the cell images, MATLAB was used for the identification of cells and calculation of cell orientation angle and cell elongation ratio. This was performed to determine whether there was a clear difference between the cells before and after the application of flow. The orientation angle calculation started first by uploading the processed images into the MATLAB code and binarizing them using the imbinarize() function if they are not already binarized in ImageJ. After this, the cells were identified as objects and measurements of orientation angles were calculated using the regionprops() function. These angles were calculated based on the x-axis, matching the direction of fluid flow from the parallel-plate experiments. For example, 0 degrees means that the cell was perfectly aligned to the direction of flow. After the calculation for orientation angles were completed for the two conditions being compared (e.g. pre-flow vs post-flow cells), the values were then plotted on a histogram for a visual analysis on the distribution angles of the cells for each condition. Elongation ratio was performed by first thresholding the image and binarizing it directly in MATLAB. This included using the graythresh() and imbinarize() function. The image was then cleaned up using the watershed() function to separate the individual objects from one another. Segmenting regions of light pixels and dark pixels into the distinct objects using the bwareaopen() function allowed us to remove any small objects that were smaller than 1000-pixel units since they were not cells. After the image clarity and object identification were completed, the elongation ratio was calculated by using the regionprops() function. This was calculated by dividing the

major axis length by the minor axis length. Once these values were calculated for both the pre-flow and post-flow conditions, the values were then plotted on a histogram for direct visual comparison of the two, as can be seen in Figure 8. The average major axis length of cells without flow was $32.04 \mu\text{m}$ with an average elongation ratio of 2.04. The average major axis length of cells after being exposed to flow was $44.72 \mu\text{m}$ with an average elongation ratio of 5.40. Comparing the two highlights how the cells post-flow had better alignment in the direction of fluid flow.

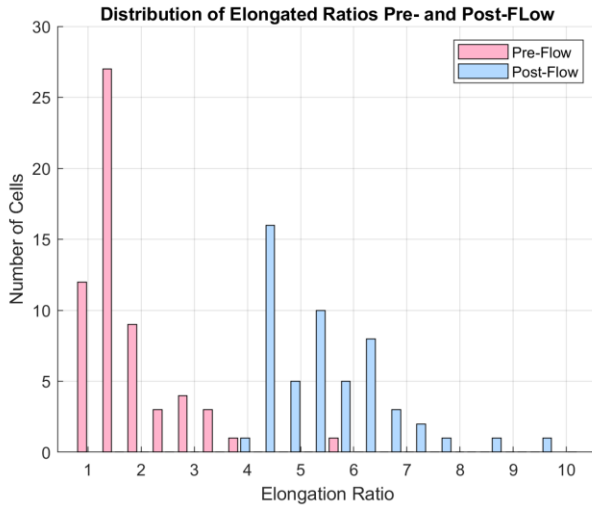


Figure 8. Histogram displaying the distribution of the cells' elongation ratios. The x-axis is the elongation ratios while the y-axis is the # of cells measured. This was calculated using the automated image analysis method using MATLAB. The orientation angle created by the MATLAB automated method used a total of 6 images for the pre-flow condition and 5 images for the post-flow condition, across 4 runs of the parallel-plate flow experiment. These images were chosen based on the ability to process them in ImageJ and the resulting clarity of the processed images in identifying the individual cells. The results of the compiled orientation angle analysis can be seen in Figure 9. The average angle of alignment for the cells before flow was -1.16 degrees with a standard deviation of 54.22 degrees. The average angle of alignment for cells after flow was -6.17 degrees with a standard deviation of 37.34 degrees. Although the manual dataset had a smaller standard deviation for the post-flow cells, the analysis both show the same result in that the pre-flow cells have a more random distribution of orientation angles with a higher standard deviation than the post-flow cells, validating the automated method of image analysis.

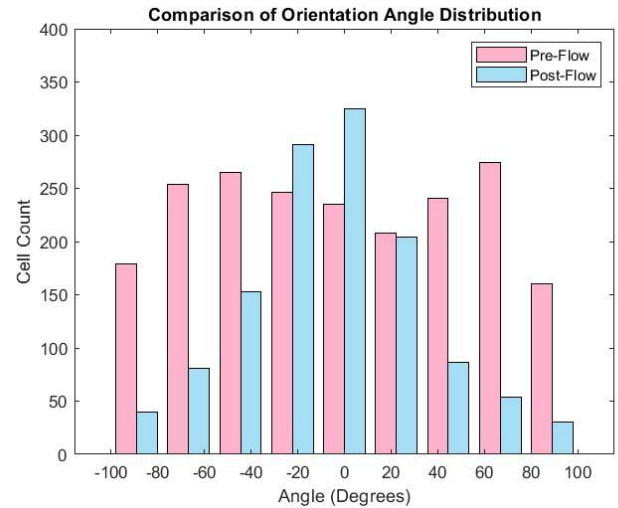


Figure 9. Histogram displaying the distribution of angle alignment of the cells relative to the direction of flow using an automated image analysis method. The x-axis is angles of alignment while the y-axis is the # of cells measured. This was calculated using the automated image analysis method using MATLAB.

To confirm the results for the flow experiments in declaring that flow results in a change in orientation angle, the same automated analysis method was run on images of control cells before and after the 24-hour period across 2 experiments. This was with the expectation that there would be random distribution throughout the entire 24-hour period, directly comparing the beginning and end. The results of the control cell analysis can be found in Figure 9. The mean angle of alignment in the start of the 24-hour period was 1.66 degrees with a standard deviation of 51.03, while the mean angle at the end of the 24-hour of -2.95 degrees with a standard deviation of 52.68. Observing Figure 10, the random distribution of both conditions can be seen, reaffirmed by the similarly large standard deviation values. Altogether, this analysis reaffirms prior literature in that flow results in cell alignment towards the direction of flow applied.

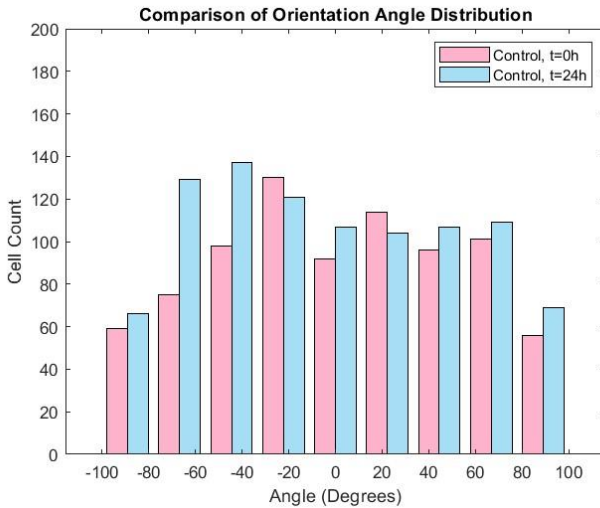


Figure 10. Histogram displaying the distribution of angle alignment of the cells relative to the direction of flow without using an automated image analysis method. The x-axis is angles of alignment while the y-axis is the # of cells measured. This was calculated using the automated image analysis method using MATLAB.

Discussion

The use of the parallel-plate flow apparatus confirmed the change in morphology in endothelial cells once they are exposed to shear stress. This aligns with previous literature, indicating that healthy endothelial cells are expected to align and elongate in the direction of flow and shear stress. In the cells' natural resting state without flow, they are presented as fully confluent, generally round, and having a cobblestone appearance. In contrast, following exposure to a shear stress of 10 dynes/cm² in the parallel-plate flow chamber, the same cells were observed to elongate and align in the direction that flow was applied. The quantitative data derived from image analysis, from Figure 3 & 4, showed a 5-fold difference between the standard deviations of the pre- and post-flow cell images for the manual method and 2-fold difference in the automated method. In addition, the average elongation ratio increased from 2.04 (1.49 manually calculated) to 5.40 (3.54 manually). Both the manual and automated calculations verify that the post-flow cells are more elongated than the pre-flow, since their ratios are farther from 1, the number which indicates a circular shape. To find this quantitative analysis, ImageJ and MATLAB were collectively used to create a quick and consistent automated method. Contrasting and binarizing images, with the exception of f-actin, allowed for the cells to be easily distinguishable and fitted for angle alignment and elongation ratio. The Directionality plugin in ImageJ allowed for f-actin fiber bundles to be accounted for

measuring the direction of a local fluorescence intensity gradient orientation and plotted the corresponding angle. MATLAB analyzed the post-processed images and created easy to understand histograms depicting stark differences in angles and elongation ratios between the pre- and post-flow cells.

These findings are particularly relevant in the realm of CCM. With lesion formation being the result of an abnormal shear stress response in the endothelial layer, it is important to understand how cells should normally adapt to shear stress, as shown in this study. The developed quantitative image analysis technique provides a tool to assess this adaptation, which can help analyze the two-dimensional adaptations of endothelial cells from cerebral blood vessels and how it can contribute to lesion formation. It also supports future studies on how mutations, such as in the KRIT-1 gene, which is linked to CCM and involved in shear stress regulated pathways, might change cell morphology and permeability.

Broader Impacts

By developing a more reliable image analysis method, CCM and its effects on cells can be studied more accurately. The parallel-plate flow system gives researchers the ability to alter certain conditions of the model, such as flow rate, shear stress, cell type and protein expression, and visualize the alignment to flow or lack thereof. The ability of this model to alter several variables can help future researchers understand what physiological and hemodynamic properties are affecting the formation of CCM in a two-dimensional apparatus.

The image analysis method developed could be used on various other cell types and protein expressions and can be used outside of flow experiments, because it is tailored to analyze a monolayer of cells no matter the experiment. Both the experiment and image analysis technique can in the future show how therapeutics interact with monolayers of cells and their tight junctions.

Limitations

In this study, the cells used were BAECs, but the cells affected by CCM are human brain microvascular endothelial cells (HBMECs). While BAECs were used because they are easy to handle and extensively researched in the past, they come from cows instead of humans. Additionally, BAECs come from aortas, meaning they are accustomed to higher shear stresses, more variability in flow, and react to different substrate properties than endothelial cells in the brain. HBMECs are the actual cell

types affected by CCM, so using these cells would more accurately represent the effects of the disease.

In imaging the monolayer of cells, confluency was important. With the images taken, depending on the density and confluency of the glass slide, it could prove difficult to decipher the boundaries of each cell in ImageJ. Each image had slightly different contrast thresholds based on the lighting of the microscope and section of the slide that was depicted. Because of this, ellipses did not fit onto every single cell in the picture. Manual manipulation with filling cells and deleting white space too small to be a cell was also done in ImageJ. The threshold for these extra pieces of debris and bubbles was created based on the pixel amount of what a standard cell in the picture was.

Future Work

The next step to further this project would be to re-run the parallel-plate flow chamber experiment with siRNA transfected BAECs knocking down KRIT-1. This gene is one of the three genes responsible for CCM1, with the phenotype caused by a “two-hit” mechanism: a congenital mutation of one allele, and a mutation of the second to produce a homozygous loss-of-function mutation¹¹. The involvement of KRIT-1 in shear stress regulated signaling pathways, and the localization of CCM lesions to low shear stress blood vessels infers that lesion formation may be a result of abnormal shear stress response of the endothelial layer, and that KRIT-1 is heavily involved¹². Analyzing cell alignment and comparing it to KRIT-1 intact cells will give greater insight on the functionality of this tight junction protein.

With the KRIT-1 knocked out BAECs as well as control BAECs, a Transendothelial Electrical Resistance (TEER) assay should be used to measure the electrical resistance across the monolayer. Resistance is inversely proportional to permeability, so if resistance is high then permeability is low, meaning there is little exchange in the blood-brain barrier¹³. Looking at the resistance of KRIT-1 knocked down and intact cells will tell how that protein affects permeability and CCM.

Materials and Methods

Cell Culture

Cells utilized in the experiment were wild-type bovine aortic endothelial cells. These were cultured and maintained using sterile BAEC complete cell culture medium comprised of Dulbecco's Modified Eagle Medium (Gibco), 4.5 g/L D-glucose, L-glutamine, without sodium pyruvate), 50 µg/mL penicillin-streptavidin, 10 percent heat-inactivated calf serum, and 2.92 mg/mL L-glutamine,

purchased from ThermoFisher. The cell culture medium was switched out every 2-3 days to ensure the cell environment was optimized, and the cells were split into separate flasks or plates once they reached a minimum of 80% confluency. For passaging, cells were rinsed with Dulbecco's phosphate-buffered saline at a pH of 7.1 without calcium or magnesium, separated with trypsin-EDTA (Gibco), and centrifuged for five minutes at 250g before being resuspended in the cell medium.

Plate Preparation

Cells prepared for the parallel-plate flow chamber experiments followed the passaging procedure and were seeded on a glass slide with a surface area of 15 cm² after the gasket was placed. Cells were plated on the slide with a 30,000 cell/cm² density and left for 2-3 days before using them in the flow experiments^{14,15}. This waiting period allowed for cells to reach ~90% confluency to ensure tight junction formation. For the parallel-plate flow experiment, two slides were seeded to have a control slide and an experimental slide.

Parallel-Plate Flow Chamber

To mimic the physiological shear stress environment found in a cerebral vein, cells were exposed to flow in a parallel-plate flow chamber. The parallel-plate flow chamber consisted of the following: a chamber piece where a slide with cells adhered on top was placed on, a peristaltic pump, a pressure damper to decrease oscillation, and cell culture medium and carbon dioxide reservoirs heated to 37 degrees Celsius in a warm water bath (Figure 1). Between the reservoir of 80 mL cell medium, the pressure damper of 30 mL medium, and the chamber that the cells were plated against, were sterilized L/S 16 PharmaPure® tubes (Cole-Parmer) connecting the system. All tubing was backfilled to eliminate air bubbles from the system before the medium circulated throughout. The chamber piece was 32 by 85 mm, made of polycarbonate plastic, and had T channels on each end that were 56.3 mm apart. Cells were plated on a 38 by 75 mm glass slide with a rectangular silicone gasket, leaving 15 cm² surface area for cells to grow to confluency on. The slide was placed face down on the polycarbonate chamber and was secured using binder clips. This set up was adapted from a previous dissertation in the lab studying CCM¹⁶.

The peristaltic pump was set at 86.7 mL/min to represent an arterial wall shear stress of 10 dynes/cm². This was chosen to represent the lower end of average arterial shear stress

and prior literature values in endothelial alignment experiments^{17,18}.

Staining Protocol

Post-flow and control slides of BAECs were stained for nuclei and f-actin. Cells were stained with a 5 µg/mL concentration of Bisbenzimidazole, fixed with 4% paraformaldehyde in PBS, permeabilized with 0.2% Triton X-100 in PBS, and stained again with a 1 µg/mL concentration of rhodamine phalloidin. They were rinsed with Dulbecco's phosphate-buffered saline at a pH of 7.1 with calcium and magnesium.

End Matter

Author Contributions and Notes

R.K and K.Q.S conducted flow experiments with the parallel-plate flow chamber and captured cell images included in this paper. They also cultured and passaged cells to maintain the cell line and took apart and cleaned the parallel-plate flow system after each use. K.Q.S stained the cells for nuclei and f-actin imaging. K.Q.S filtered and binarized images on ImageJ and manually collected angle and elongation ratio data for the introduction. R.K created MATLAB code to produce histograms comparing angles of alignment for edited images. K.Q.S collected elongation ratio data from edited images. K.Q.S wrote the Abstract, Introduction, and Parallel-Plate and ImageJ sections for the Results, and Discussion. K.Q.S. and R.K wrote the MATLAB section of Results. R.K and K.Q.S both wrote the Materials and Methods section.

The authors declare no conflict of interest.

Acknowledgments

We would like to thank the UVA Biomedical Engineering Department, Dr. Timothy Allen, and the Capstone teaching team for their support and for making this project possible through our Capstone course. We would like to thank our advisor, Dr. Brian Helmke, for introducing us to this project, for teaching us related concepts, protocols, and laboratory skills, and for providing us with many of the necessary resources to perform these experiments. We would also like to thank Grace Ford, our mentor, for teaching us about parallel-plate flow systems, cell culturing, and cell staining, and for repeatedly making time to help us with unfamiliar protocols. Figure 1 was created with Biorender.com.

References

1. Awad, I. A., & Polster, S. P. (2019). Cavernous angiomas: Deconstructing a neurosurgical disease. *Journal of Neurosurgery*, 131(1), 1–13. <https://doi.org/10.3171/2019.3.JNS181724>
2. Zafar, A., Quadri, S. A., Farooqui, M., Ikram, A., Robinson, M., Hart, B. L., Mabray, M. C., Vigil, C., Tang, A. T., Kahn, M. L., Yonas, H., Lawton, M. T., Kim, H., & Morrison, L. (2019). Familial Cerebral Cavernous Malformations. *Stroke*, 50(5), 1294–1301. <https://doi.org/10.1161/STROKEAHA.118.02231>
3. Cavernous Malformations. (2019, May 13). Johns Hopkins Medicine. <https://www.hopkinsmedicine.org/health/condition-s-and-diseases/cavernous-malformations>
4. Pagenstecher, A., Stahl, S., Sure, U., & Felbor, U. (2009). A two-hit mechanism causes cerebral cavernous malformations: Complete inactivation of CCM1, CCM2 or CCM3 in affected endothelial cells. *Human Molecular Genetics*, 18(5), 911–918. <https://doi.org/10.1093/hmg/ddn420>
5. Li, J., Zhao, Y., Coleman, P., Chen, J., Ting, K. K., Choi, J. P., Zheng, X., Vadas, M. A., & Gamble, J. R. (2019). Low fluid shear stress conditions contribute to activation of cerebral cavernous malformation signalling pathways. *Biochimica Et Biophysica Acta. Molecular Basis of Disease*, 1865(11), 165519. <https://doi.org/10.1016/j.bbadis.2019.07.013>
6. Girard, P. R., & Nerem, R. M. (1995). Shear stress modulates endothelial cell morphology and F-actin organization through the regulation of focal adhesion-associated proteins. *Journal of Cellular Physiology*, 163(1), 179–193. <https://doi.org/10.1002/jcp.1041630121>
7. Nerem, R. M. (1991). Shear force and its effect on cell structure and function. *ASGSB Bulletin: Publication of the American Society for Gravitational and Space Biology*, 4(2), 87–94.
8. Xu, F., Beyazoglu, T., Hefner, E., Gurkan, U. A., & Demirci, U. (2011). Automated and Adaptable Quantification of Cellular Alignment from Microscopic Images for Tissue Engineering Applications. *Tissue Engineering. Part C, Methods*, 17(6), 641–649. <https://doi.org/10.1089/ten.tec.2011.0038>
9. Sauvola, J., & Pietikäinen, M. (2000). Adaptive document image binarization. *Pattern Recognition*, 33, 225–236. [https://doi.org/10.1016/S0031-3203\(99\)00055-2](https://doi.org/10.1016/S0031-3203(99)00055-2)

10. Dragich, A., McClendon, M., Hadi, S., Velez-Ortega, A. C., & Frolenkov, G. I. (2024). High-Resolution Focused-Ion Beam Scanning Electron Microscopy Reveals Differentially Organized F-actin Compartments in Cochlear Hair Cell Stereocilia: 82nd Annual Meeting Microscopy Society of America and the 58th Annual Meeting Microanalysis Society, M and M 2024. *Microscopy and Microanalysis*, 30(2024), 973–974. <https://doi.org/10.1093/mam/ozae044.479>
11. Pagenstecher, A., Stahl, S., Sure, U., & Felbor, U. (2009). A two-hit mechanism causes cerebral cavernous malformations: Complete inactivation of CCM1, CCM2 or CCM3 in affected endothelial cells. *Human Molecular Genetics*, 18(5), 911–918. <https://doi.org/10.1093/hmg/ddn420>
12. Li, J., Zhao, Y., Coleman, P., Chen, J., Ting, K. K., Choi, J. P., Zheng, X., Vadas, M. A., & Gamble, J. R. (2019). Low fluid shear stress conditions contribute to activation of cerebral cavernous malformation signalling pathways. *Biochimica Et Biophysica Acta. Molecular Basis of Disease*, 1865(11), 165519. <https://doi.org/10.1016/j.bbadis.2019.07.013>
13. Swamy, H., & Glading, A. J. (2022). Contribution of protein–protein interactions to the endothelial-barrier-stabilizing function of KRIT1. *Journal of Cell Science*, 135(2), jcs258816. <https://doi.org/10.1242/jcs.258816>
14. Abo-Aziza, F. A. M., & A.A, Z. (2017). The Impact of Confluence on Bone Marrow Mesenchymal Stem (BMMSC) Proliferation and Osteogenic Differentiation. *International Journal of Hematology-Oncology and Stem Cell Research*, 11(2), 121–132.
15. Animal Cell Culture Guide | ATCC. American Type Culture Collection. (n.d.). <https://www.atcc.org/resources/culture-guides/animal-cell-culture-guide>
16. Mott, R. E. (2008). *The Endothelial Mechanoreponse: Dynamic Mechanochemical Mechanisms at the Cell-matrix Interface*. Charlottesville, VA: 2008.
17. Buchanan, C. F., Verbridge, S. S., Vlachos, P. P., & Rylander, M. N. (2014). Flow shear stress regulates endothelial barrier function and expression of angiogenic factors in a 3D microfluidic tumor vascular model. *Cell Adhesion & Migration*, 8(5), 517–524. <https://doi.org/10.4161/19336918.2014.970001>
18. Davies, P. F., Robotewskyj, A., & Griem, M. L. (1994). Quantitative studies of endothelial cell adhesion. Directional remodeling of focal adhesion sites in response to flow forces. *The Journal of Clinical Investigation*, 93(5), 2031–2038. <https://doi.org/10.1172/JCI117197>